A multispectral, high-speed, low-cost device in the UV-MWIR spectral range

Thomas Svensson*, Roland Lindell, Leif Carlsson
Swedish Defence Research Agency, FOI
P.O.Box 1165, SE-58111 Linköping, Sweden
* thosve@foi.se; phone: +4613378093

ABSTRACT

This paper presents the design and performance of a multispectral, high-speed, low-cost device. It is composed of six separate single element detectors covering the spectral range from UV to MWIR. Due to the wide spectral ranges of the detectors, these are used in conjunction with spectral filters.

The device is a tool to spectrally and temporally resolve large field of view angularly integrated signatures from very fast events and get a total amplitude measure. One application has been to determine the maximal amplitude signal in muzzle flashes. Since the pulse width of a muzzle flash is on the order of 1 ms, a sensor with a bandwidth significantly higher than 1000 Hz is needed to resolve the flash. Examples from experimental trials are given.

Keywords: multispectral, high-speed, low-cost, muzzle flash detection

1. INTRODUCTION

Driving issues for reconnaissance and warning systems are improved detection of low signature objects, larger range capabilities, shorter reaction times and improved robustness against decoys and false alarms. In order to reach these objectives, key features have to be identified like spatial, spectral and temporal resolution, wavelength range and angular coverage. Signatures therefore have to be measured over the full spectral region from UV to the thermal infrared with high temporal resolution. Data collected from multispectral, imaging cameras give the possibility to evaluate temporal, spectral, spatial and dynamic target signature features. Multispectral registrations allow spectral properties of targets and clutter to be investigated in real time. Which features that mainly will contribute with the information that leads to the detection of a target will depend both on the target and the background properties. The spectral region being selected is a compromise between the spectral signatures of the target and the size, weight, cost and power consumption of the sensor.

Increasing the resolution of a feature will increase the detection probability due to the increase of information in the collected sensor data, but the resolution of signature features can only be increased to an upper limit determined by the data transport capacity and/or the data storage capacity of the system. A solution is then to increase the resolution of the feature under interest and decrease the resolution in the other. An example is missile warning systems, which require wide field of view sensors. A high spatial resolution allows small targets like missiles to be distinguished from extended targets and facilitates location of the target. A high spatial resolution however corresponds to a low angular coverage. In a corresponding way, high frame rates facilitates high temporal resolution of the different stages characteristic for a missile launch such as ejection phase, boost phase and sustain phase, engine instabilities and atmospheric turbulence properties. High frame rates are reached by sub-windowing and a decrease of the spatial coverage. Another example is gunshot signatures, which are demanding to identify, locate and process due to that muzzle flashes are very fast events with a duration of about 1 ms. A sensor with a frame rate significantly higher than 1000 Hz is then needed to detect the flash, which is beyond the frame rate of an infrared imaging sensor.

Frame rates significantly higher than 1000 Hz can be reached with single element detectors. Multispectral measurements with high-speed single radiometers has been demonstrated [1, 2]. In this paper we present a low-cost setup with six single element detectors covering the UV-MWIR spectral range. Due to the wide spectral ranges of the detectors, these are used in conjunction with spectral filters to attain a spectral resolution $\Delta\lambda/\lambda < 0.5$ to acquire the spectral characteristics. The sampling is simultaneous in the spectral bands, which is required to fully identify the wavelength dependent temporal properties of fast optical signals. The high-speed multispectral device has been used to study very fast events like the development of explosions and muzzle flashes, and separate the different phases in the different

Optical Design and Engineering IV, edited by Laurent Mazuray, Rolf Wartmann, Andrew Wood, Jean-Luc M. Tissot, Jeffrey M. Raynor, Proc. of SPIE Vol. 8167, 816725 · © 2011 SPIE · CCC code: 0277-786X/11/$18 · doi: 10.1117/12.897121

wavelength bands. Data from the UV-MWIR spectral range yields usable signatures for detection of high-temperature targets. The MWIR spectral range has been used for detection of muzzle flashes since the 1960s [3-4]. One specific goal in the development of muzzle flash detection systems has been to keep the costs low. The detector technology is then an important parameter. Uncooled systems have several cost-effective potentials. A low-cost detection system based on CMOS sensor technology in the SWIR range has been proposed [5]. The SWIR wavelength band (ca 1-3 μm) have several advantages in operational 2D imaging systems, e.g. good imaging quality [6]. A detector technology in the SWIR band is InGaAs (0.9-1.7 μm), which is a high-speed detector with theoretical bandwidths of 75 GHz or higher [7].

Though the total costs for the device presented have been kept low by a simple design and a basic radiometric characterization, it has shown to be a powerful tool to evaluate temporal and spectral properties of fast events. In muzzle flash studies the six single element device has been part of a 3-step process. In a first step the emission is recorded with high temporal resolution in the six spectral bands. In a second step, the range capabilities are studied in selected spectral bands using an imaging system with a high frame rate and a high spatial resolution. In a third step, based on previous results, the range capability is then studied using cost-effective sensors with tactical field of views.

2. TECHNICAL DESCRIPTION

2.1. Detectors

Specifications of the six selected single element detectors (Thorlabs) are according to Table 1. One of the detectors is shown in Figure 1. A typical spectral responsivity curve for the detector is shown in the same figure.

To avoid saturation of the detectors and acquire data with a proper signal-to-noise ratio the detectors 0, 1, 2, 3 and 4 are provided with eight-position rotary switches. These allow the gain setting to be varied from 0 dB up to 70 dB in 10 dB steps. The setting 0 dB corresponds to a gain ca $1.51 \cdot 10^3$ V/A and 70 dB to a gain ca $4.75 \cdot 10^6$ V/A. For the detectors 0, 1 and 2 the gain will however also affect the bandwidth, which goes from 1 MHz (or higher) at 0 dB down to 10 kHz at 70 dB (the gain and the bandwidth are inversely proportional). For detector 3 and detector 4, the gain and the bandwidth can be set independent of each other (between 0 – 70 dB and 500 Hz – 1 MHz resp.). The possibilities to adjust the signal level by varying the gain can be used in combination with external ND filters, which reduce the incident radiance level on the detector.

Table 1. Specifications of the six single element detectors.

Det	Thorlabs no:	Material	Spectral range [μm] *)	Cooling	Resp [ns]	Electr. bandwidth (up to)
0	PDA25K	GaP	0.15 – 0.55	-	46.6	7.5 MHz
1	PDA36A	Si	0.35 – 1.10	-	20.6	17 MHz
2	PDA10CS	InGaAs	0.70 – 1.80	-	20.6	17 MHz
3	PDA10DT	InGaAs	1.20 – 2.57	Thermoelectric	350	1 MHz
4	PDA10DT	InGaAs	1.20 – 2.57	Thermoelectric	350	1 MHz
5	PDA20H	PbSe	1.50 – 4.80	-	35000	10 kHz

*) Spectral range before filtering

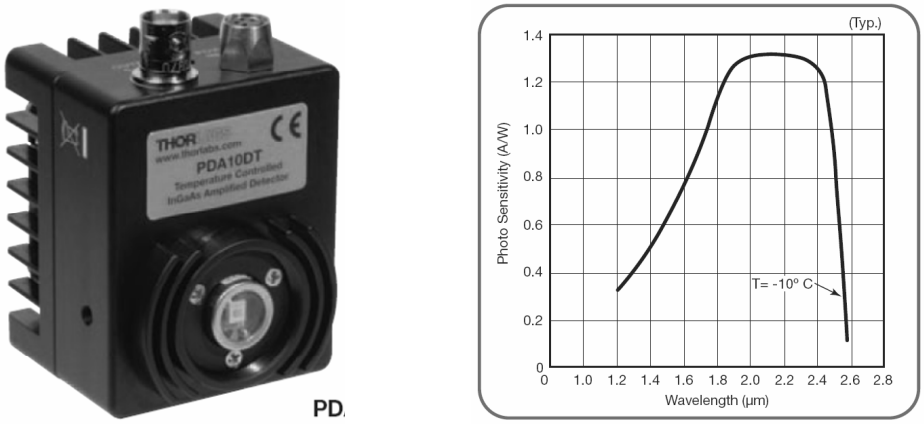

Figure 1. To the left a typical single element detector (PDA10DT, see Table 1) and to the right the corresponding responsivity.

2.2. Spectral filters

The measured transmission for the filters (Spectrogon) used for the different detectors are according to Table 2. In Table 2 are also stated the spectral ranges of selected detector and filter combinations. Filter characteristics for two of the filters (filter 3, 1456 nm – 1490 nm, and filter 4, 2128 nm – 2565 nm) are shown in Figure 2.

Table 2. Typical transmission for the filters (Spectrogon) used in conjunction with the detectors 0 - 5. The spectral ranges of detector and filter combinations are according to the right column.

Det. no:	Filter type	Lower Wavelength	Upper Wavelength	Average transmission	Spectral range of detector + filter [µm]
0	Short pass	-	288 nm		0.15 – 0.29
1	Short pass	-	646 nm	90 %	0.35 – 0.65
2	Band pass	790 nm	1370 nm	65 %: 790 – 920 nm 85 %: 920–1370 nm	0.79 – 1.37
3	Band pass	1456 nm	1790 nm	91 %	1.46 – 1.79
4	Band pass	2128 nm	2565 nm	89 %	2.13 – 2.57
5	Long pass	3004 nm	-	86 %	3.00 – 4.80

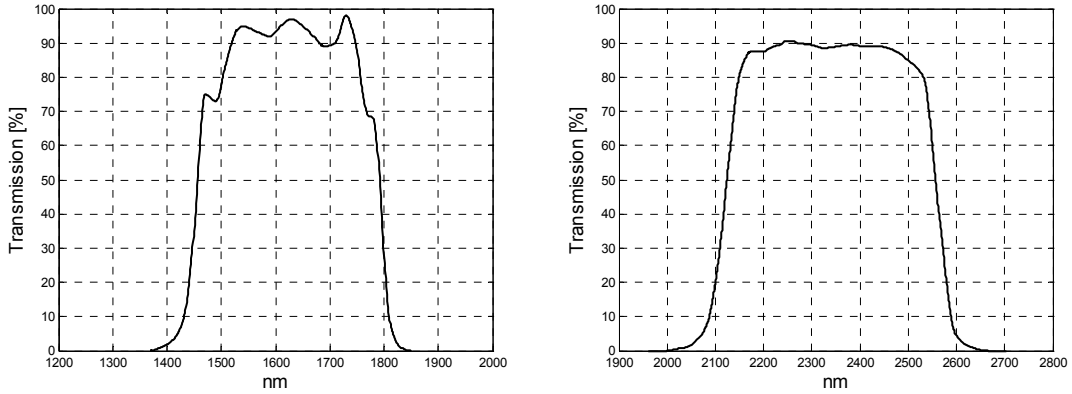

Figure 2: The spectral transmission for the filters used in conjunction with detector 3 (left) and detector 4 (right).

2.3. Mounting

The single element detectors are mounted on a common fixture together with a small TV-camera to monitor the sensors direction (Figure 3). The field of view (FOV) for the six single element detectors is individually defined by a mounted tube in front of the detector element and the actual position of the active element. The calculated FOV's for the detectors are shown in Table 3.

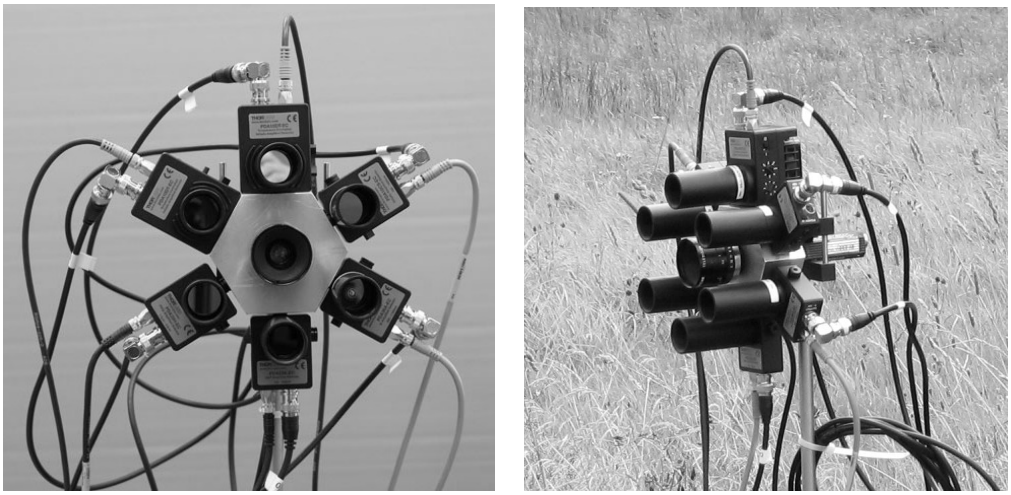

Figure 3. The 6-pack composed of six detectors. A small TV-camera is placed in the middle to monitor the sensors direction. The FOV is individually defined by a mounted tube in front of each single detector element (Table 3).

Table 3. Size of active area and calculated FOV for the six single element detectors.

Detector no:	Detector area [mm]	FOV [°]
0	2.54 x 2.54	21.3
1	3.6 x 3.6	21.0
2	Ø 1.0	21.6
3	Ø 1.0	23.3
4	Ø 1.0	23.3
5	2.0 x 2.0	21.4

2.4. Data acquisition

The signals from the six channels are measured using a NI PCI-6133 multifunction data acquisition (DAQ) board, featuring a dedicated analog-to-digital converter (ADC), 14 bit (National Instruments). It is used with the interactive data-logging software LabVIEW SignalExpress. Up to 8 analog inputs can be sampled simultaneously with up to 2.5 MS/s/channel (MS=megasample).

3. RADIOMETRIC CHARACTERIZATION

Radiometric calibrations of sensors 1 to 4 were carried out using an integrating sphere SR-3B (Sphere-Optics) as a reference source. The incident power ϕ [W] on the detector element is given by

$$\phi = \Omega_{IFOV} \cdot A \cdot \int \tau_{Filter}(\lambda)\left[L_{Sphere}(\lambda)\tau_{Atm}(\lambda) + L_{Atm}(\lambda)(1-\tau_{Atm})\right] d\lambda \quad (1)$$

where Ω_{IFOV} is the solid angle defined by the mounted tube = $\pi/4 \cdot \theta^2_{IFOV}$, A = the detector area, $\tau_{Filter}(\lambda)$ = the spectral transmission of the filter, $L_{Sphere}(\lambda)$ = the spectral radiance at the exit port of the sphere, $\tau_{Atm}(\lambda)$ = the spectral atmospheric transmission and $L_{Atm}(\lambda)$ = the spectral atmospheric radiance.

If the reference source and the target are measured at short ranges, the atmosphere can be expected to be of minor importance. By disregarding the atmospheric influence and approximating $\tau_{Filter}(\lambda)$ with a boxcar function, (1) is simplified into

$$\phi = \Omega_{IFOV} \cdot A \cdot \overline{\tau}_{Filter} \int_{\lambda_1}^{\lambda_2} L_{Sphere}(\lambda) d\lambda \quad (2)$$

where $\overline{\tau}_{Filter}$ is the average transmission of the filter, given in Table 2. The detected power is converted to an electrical voltage, U [V]

$$U = \Omega_{IFOV} \cdot A \cdot \overline{\tau}_{Filter} \int_{\lambda_1}^{\lambda_2} L_{Sphere}(\lambda) R_{Detector}(\lambda) d\lambda \quad (3)$$

$R_{Detector}(\lambda)$ is the detector responsivity, expressed by $R_{Detector}(\lambda) = R_{Peak} \times R_{Norm}(\lambda)$

$$U = R_{Peak} \cdot \Omega_{IFOV} \cdot A \cdot \bar{\tau}_{Filter} \int_{\lambda_1}^{\lambda_2} L_{Sphere}(\lambda) R_{Norm}(\lambda) d\lambda \quad (4)$$

$R_{Norm}(\lambda)$ is the spectral detectivity normalized to the peak value. The numerical size of R_{Peak} [DN·W^{-1}] is determined in the radiometric calibration.

The registered output voltage in (4) will depend on the gain setting of the detectors. Figure 4 shows examples of calibration curves. The mean response of pixels in an array is typically linear over a substantial dynamic range, while the response of a single detector element tends to be non-linear [8]. The linearities of the detector's radiometric responses were therefore investigated by measuring the sphere source at ≥ 3 radiance levels.

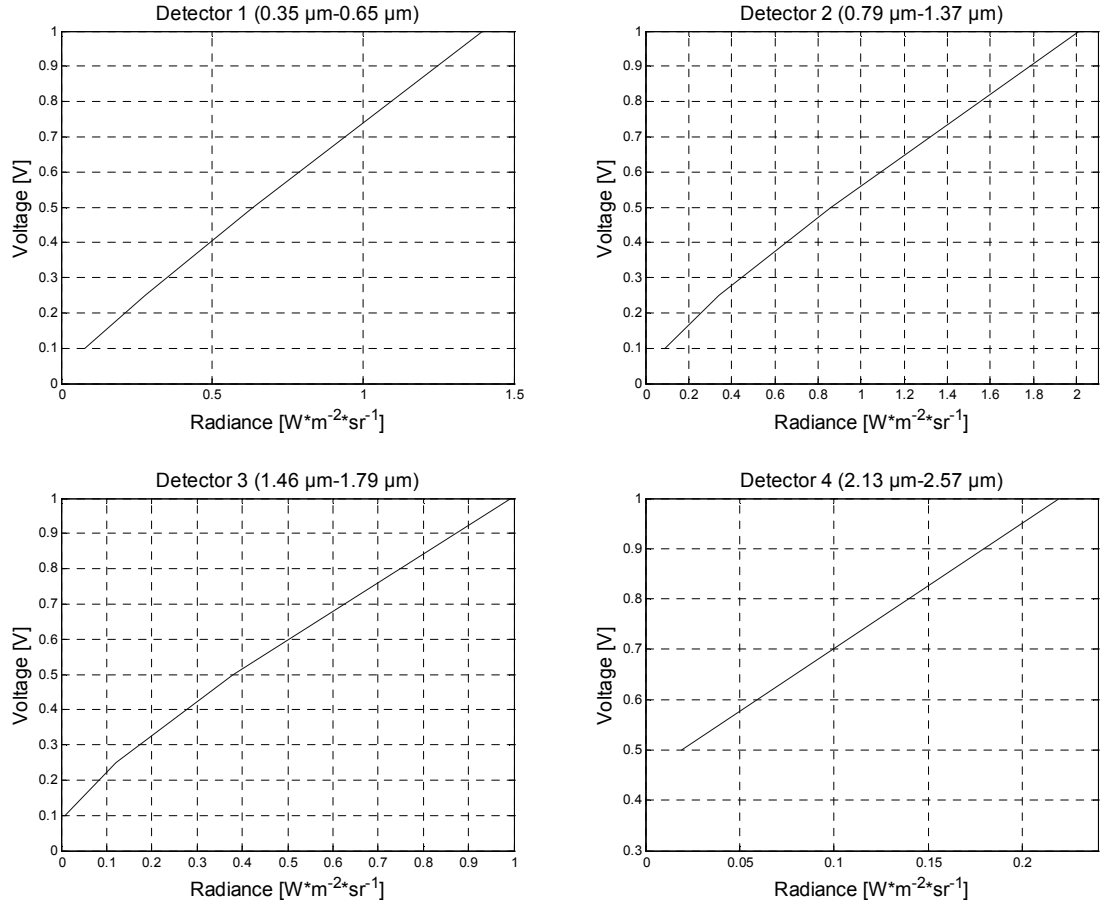

Figure 4. Calibration curves for sensor 1-4; the output from the detector [V] is displayed as a function of the incident radiance [W·m^{-2}·sr^{-1}].

Responsivities R_V [V/W] for the detectors 1-4, calculated by $\Delta U/\Delta\phi$, are shown in Table 4. Detector 0 and 5 have not been separately calibrated. Instead the responsivities stated in data sheets were used. In the same table are shown estimated RMS levels of the noise [mV].

Table 4. Responsivities and RMS levels of noise for detector 0-5.

Detector no:	Spectral range of detector+filter [µm]	Responsivity R_V [V/W]	RMS noise [mV]
0	0.15 – 0.29	$2 \cdot 10^5$	1.2
1	0.35 – 0.65	$5.2 \cdot 10^5$	0.58
2	0.79 – 1.37	$5.9 \cdot 10^6$	0.90
3	1.46 – 1.79	$9.4 \cdot 10^6$	0.60
4	2.13 – 2.57	$2.7 \cdot 10^7$	0.67
5	3.00 – 4.80	$2 \cdot 10^5$	11

With calibration data and the FOV's given in Table 3, the measured signature in each waveband can be transformed into a radiometric unit like intensity [W/sr]. Disregarding the atmospheric influence, the intensity is given by

$$I_{Target} = \Omega_{IFOV} \cdot R^2 \cdot L_{Target} \quad (5)$$

where L_{Target} = the measured radiance, Ω_{IFOV} = the solid angle defined by the mounted tube and R = the distance between the detector and the target.

4. MEASUREMENTS

An example with results from a muzzle flash detection trial is presented below.

The measurement setup is shown in Figure 5. The distance between the multispectral sensor and the barrels was varied between 7-14 meters according to the figure. The analysis was carried out for the six single element detectors without considering how much of the detectors FOV was covered by the muzzle flash.

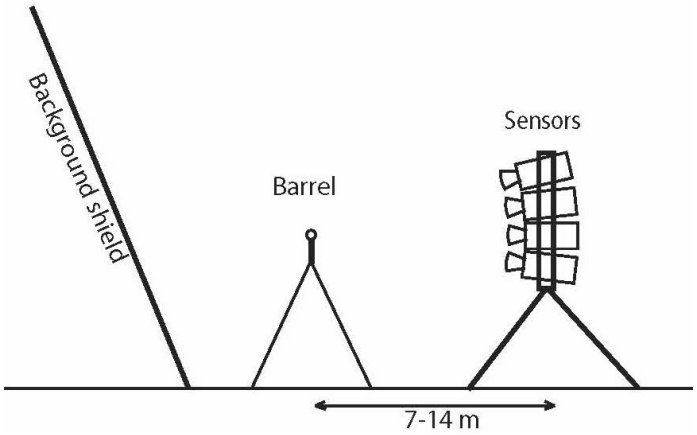

Figure 5. The measurement setup with barrels, sensors and background shield. The shooting direction was ca 90°.

Data from the six detector element device were collected during 3 s. The sampling rate in each channel was 10000 Hz. A time diagram of a flash in the spectral band nr 4 is shown below (Figure 6).

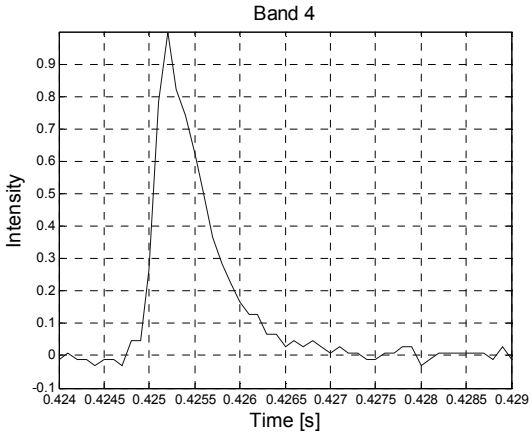

Figure 6: Band 4 (2.13-2.57 μm); the figure shows a registration of a muzzle flash during 5 ms. The registered intensity has been normalized to the peak value. The same registration during 40 ms is shown in the figure below.

In Figure 7 is shown the variation in the time diagrams between the wavelength bands 1, 3, 4 and 5.

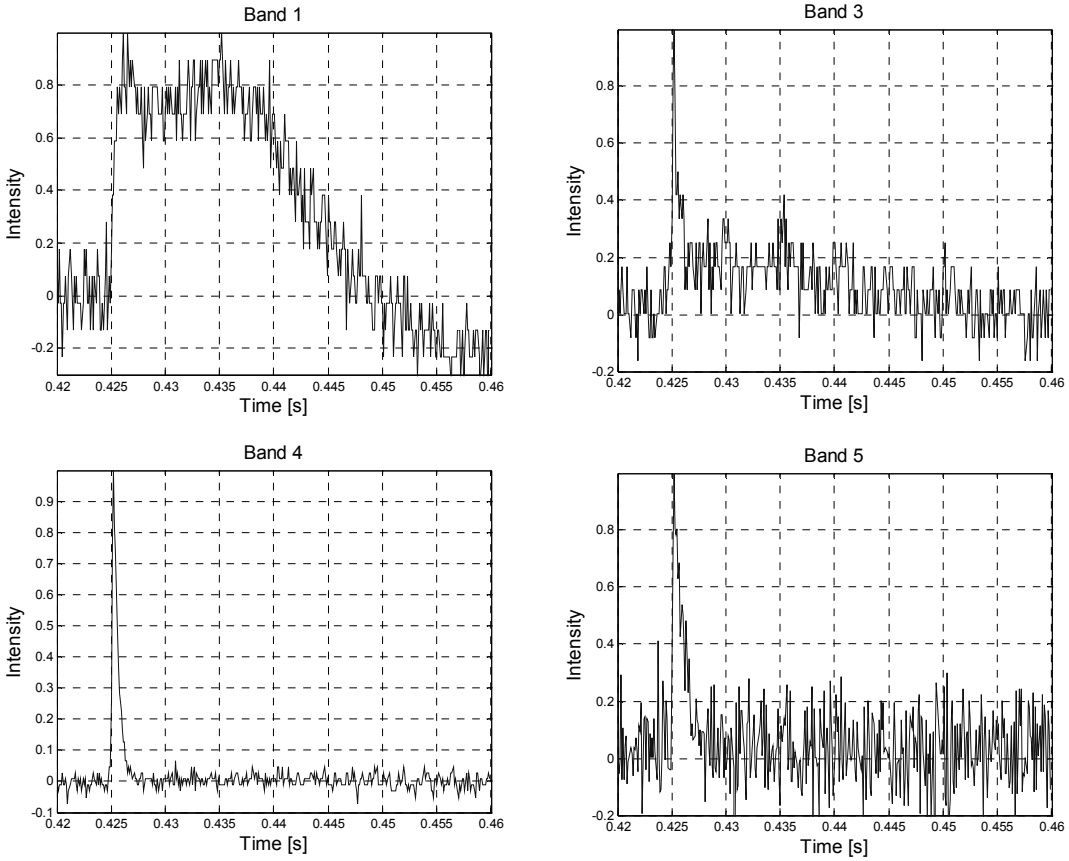

Figure 7. Time diagrams for band 1 (0.35 μm-0.65 μm) , 3 (1.46 μm-1.79 μm), 4 (2.13 μm-2.57 μm) and 5 (3.00 μm-4.80 μm). The registered intensity, normalized to the peak value, is shown as a function of time [s] during 40 ms. A scattering flow field (scattered solar radiation) is seen in band 1 after the flash. The reason to the baseline drift (0 to -0.2) is not clear.

5. CONCLUSIONS

To spectrally and temporally resolve very fast optical signals, e.g. explosions, is demanding due to short durations and short rise times. Bandwidths significantly higher than 1000 Hz may be needed. The wavelength range and the spectral resolution have to be carefully considered, depending on the characteristics of the optical signal.

We have presented a multispectral, high-speed, low-cost device with six spectral wavebands. The device covers the UV-MWIR spectral range with a spectral resolution $\Delta\lambda/\lambda < 0.5$. The six channels are sampled simultaneously, which is required to fully identify the wavelength dependent temporal properties of fast optical signals. The total costs for the device have been kept low by a simple design and a basic radiometric characterization. The high-speed multispectral device has shown to be a powerful tool to evaluate temporal and spectral properties of very fast events

6. REFERENCES

[1] A.D.Devir, M.Y.Engel, I.Mendelewicz, S.Vilan, D.Cabib, A.Gil, *Fast Multi Channel Radiometer for Diagnosing Munition Flashes*, Proc. of SPIE, Vol.6940 (2008)

[2] D.B.Law, E.M.Carapezza, C.J.Csanadi, G.D.Edwards, T.M.Hintz, R.M.Tong, *Multi-spectral signature analysis measurements of selected sniper rifles and small arms*, Proc. of SPIE Vol.2938 (1997)

[3] G. Klingenberg, J.Heimerl, *Gun Muzzle blast and flash*, Progress in Astronautics, 139, AIAA (1992)

[4] S.Carfagno et.al. *Engineering design handbook, Spectral Characteristics of Muzzle Flash*, US Army Material Command, Washington DC (1967)

[5] A.Voskoboinik, *Novel approach for low-cost muzzle flash detection system*, Proc. of SPIE Vol.6940 (2008)

[6] J.Battaglia, R.Brubaker, M.Ettenberg, D.Malchow, *High speed Short Wave Infrared (SWIR) imaging and range gating cameras*, Proc. of SPIE Vol.6541 (2007)

[7] E.L.Dereniak, G.D.Boreman. *Infrared detectors and systems*, John Wiley & Sons, Inc. (1996)

[8] W.Isoz, T.Svensson, I.Renhorn, "*Nonuniformity correction of infrared focal plane arrays*", Proc. SPIE Vol. 5783, Infrared technology and applications XXXI (2005)